Geometrical feature of the scaling behavior of the limit-point pressure of inflated hyperelastic membranes

Ganesh Tamadapu,[*] Nikhil Nandkumar Dhavale,[†] and Anirvan DasGupta[‡]

Department of Mechanical Engineering and Centre for Theoretical Studies, Indian Institute of Technology Kharagpur,
Kharagpur-721302, India

The occurrence of the limit-point instability is an intriguing phenomenon observed during stretching of hyperelastic membranes. In toy rubber balloons, this phenomenon may be experienced in the sudden reduction in the level of difficulty of blowing the balloon accompanied by its rapid inflation. The present paper brings out a link between the geometry and strain-hardening parameter of the membrane, and the occurrence of the limit-point instability. Inflation of membranes with different geometries and boundary conditions is considered, and the corresponding limit-point pressures are obtained for different strain-hardening parameter values. Interestingly, it is observed that the limit-point pressure for the different geometries is inversely proportional to a geometric parameter of the uninflated membrane. This dependence is shown analytically, which can be extended to a general membrane geometry. More surprisingly, the proportionality constant has a power-law dependence on the nondimensional material strain-hardening parameter. The constants involved in the power-law relation are universal constants for a particular membrane geometry.

PACS number(s): 46.70.−p, 46.90.+s, 46.25.Cc

I. INTRODUCTION

The membranes used in membranes and inflatable structures are usually made of polymeric materials (such as rubber) which are highly nonlinear, and modeled as hyperelastic materials (see, e.g., [1–4]). During inflation, a membrane undergoes large deformation, which makes the analysis geometrically nonlinear as well (see, e.g., [5–11]). It is the interaction of the material and geometric nonlinearities that exhibits counterintuitive and surprising effects, some of which have been referenced above (also see, [12,13]).

Nonlinear materials exhibit various interesting (but incompletely understood) phenomena when stretched. In this respect, critical points, which are usually defined with respect to a load or stretch parameter, are of particular interest. Critical points are mainly classified as bifurcation points and limit points. At a bifurcation point, there coexists more than one equilibrium solution branch. Beyond this point, only the stable solution branch is expressed. At the limit point, which will be our focus here, the load or stretch parameter itself exhibits a limiting (locally extremal) behavior. Thus the configuration of the membrane in the vicinity of the limit point becomes nonunique in terms of the load or stretch parameter.

Interesting observations during balloon inflation experiments have been reported in the past [7,14–17]. The key point noted in most of these observations is the occurrence of the limit-point instability. This intriguing phenomenon observed in toy balloons has important consequences for any internally pressurized or stretched membranes. Such membranes abound in nature in the form of biological membranes. In recent times, inflatable structures have become very common. Applications are found in terrestrial and space structures [18], and vibration or impact isolation and damping devices such as inflated tires and air bags.

During inflation past the limit point, a structure can undergo rapid deformation or inflation (with the possibility of bursting) accompanied with a drop in the pressure. Physically, the structure may become marginally controllable at such points. Hence, estimation of limit points is important for predicting the behavior of inflated or loaded membrane structures. The value of the critical load or pressure at the limit point seems to be related to the material property. However, it also has a geometry dependence, which has remained unnoticed. These issues provide a motivation for the present study.

In this paper, a study has been carried out on the inflation of axisymmetric membranes of different geometries and boundary conditions focusing, in particular, on the limit-point instability phenomenon and its connection to the geometry of the membranes. Our objective is to bring out a link between the geometry and material parameters of the membrane, and the occurrence of the limit-point instability during inflation. The strain energy for the hyperelastic membrane material is taken in the Mooney-Rivlin form with both strain-hardening and softening behavior [19]. It is found that the limit-point pressure of a membrane is inversely proportional to its geometric parameter in the unstretched state. This behavior can be understood analytically for membranes of any geometry. Remarkably, the proportionality constant exhibits a power-law behavior in terms of the strain-hardening parameter of the membrane, and involving two universal constants which are solely dependent on the particular geometry of the membrane.

The paper is organized as follows. In Sec. II, the kinematics of deformation of an axisymmetric membrane has been discussed. The variational formulation of the inflation problem has been presented in Sec. III. Various axisymmetric geometries and the corresponding equilibrium equations and the boundary conditions are discussed in Sec. IV. The numerical results are presented in Sec. V. The paper is concluded with Sec. VI, wherein some future directions are also indicated.

———————

[*]ganesh@cts.iitkgp.ernet.in
[†]nikhil.dhavale@gmail.com
[‡]anir@mech.iitkgp.ernet.in
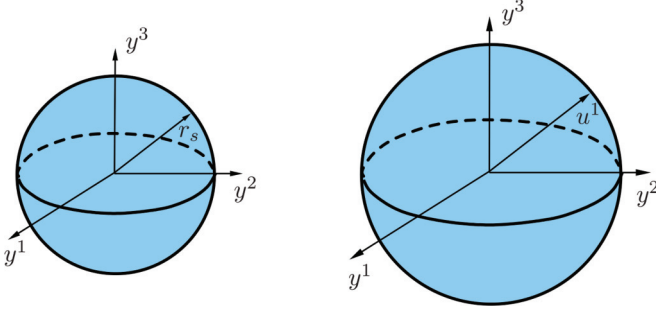
FIG. 1. (Color online) Spherical membrane before inflation and after inflation.

II. KINEMATICS OF DEFORMATION

Consider a homogeneous, isotropic, hyperelastic axisymmetric membrane with convected coordinates on the surface as x^1 (radial or meridional) and x^2 (circumferential) (see Figs. 1, 3, and 6). Let x^3 be the coordinate along the local normal, with $x^3 = 0$ representing the midsurface of the membrane. Axisymmetric deformation of the membrane is assumed in the analysis. Let g_{ij} and $\tilde{g}_{ij}$ be the undeformed and the deformed metric tensors of the membrane. The position vector of a point on the deformed membrane is given by $p^i = y^i + x^3 \lambda_3 n^i$, where y^i is the position vector of a point on the midsurface, λ_3 is the principal stretch along the surface normal to the membrane, and n^i is the unit outward normal vector to the membrane midsurface given by

$$n^i = \tfrac{1}{2}\delta^{il}\varepsilon^{\alpha\beta}\varepsilon_{ljk}y^j_{,\alpha}y^k_{,\beta}, \qquad \text{(summation convention)} \quad (2.1)$$

where $\varepsilon^{\alpha\beta} = e^{\alpha\beta}/\sqrt{\tilde{g}}$ [$\tilde{g} = \det(\tilde{g}_{\alpha\beta})$] and $\varepsilon_{ijk} = e_{ijk}$ are, respectively, the completely antisymmetric contravariant (in two-dimensional curvilinear coordinates) and covariant (in three-dimensional Euclidean space) Levi-Civita tensors. Here, $e^{\alpha\beta}$ and e_{ijk} are the permutation symbols, and $y^i_{,\alpha} = \partial y^i/\partial x^\alpha$ are the two orthogonal vectors on the tangent plane of the deformed membrane surface. The eigenvalues of the right Cauchy-Green deformation tensor $C^i_{\ j} = g^{ik}\tilde{g}_{kj}$ are, say λ_i^2 ($i = 1,2,3$), where λ_1 and λ_2 are the in-plane principal stretches of the membrane.

III. VARIATIONAL FORMULATION

A. Material Strain Energy

For a homogeneous and isotropic generalized Mooney-Rivlin solid, the strain energy density function (per unit undeformed volume) may be expressed as [20]

$$\hat{V} = C_1(\tilde{I}_1 - 3) + C_2(\tilde{I}_2 - 3) + \tfrac{1}{2}K_1(J - 1)^2, \quad (3.1)$$

where $C_1, C_2,$ and K_1 are the material properties, and $J = \sqrt{\det(C^i_{\ j})}$, $\tilde{I}_1 = J^{-2/3}I_1$, and $\tilde{I}_2 = J^{-4/3}I_2$. This rubber elasticity model is used for limited compressible materials with $K_1 \gg 2C_1$. Here, $I_1, I_2,$ and I_3 are the strain invariants of the deformation tensor $C^i_{\ j}$ given by $I_1 = C^i_{\ i}$, $I_2 = \frac{1}{2}(C^i_{\ i}C^j_{\ j} - C^i_{\ j}C^j_{\ i})$, $I_3 = \det(C^i_{\ j})$. For a nearly incompressible material with small strain limit, the material properties $C_1, C_2,$ and K_1 can be related to the familiar bulk modulus (K) and shear modulus (μ) as $\mu = 2(C_1 + C_2)$ and $K = 2K_1$. For an incompressible material, we have $I_3 = \lambda_3^2\tilde{g}_s/g_s = 1$, implying

$\lambda_3^2 = g_s/\tilde{g}_s$, where g_s and $\tilde{g}_s$ are, respectively, the surface metric determinants in the undeformed and deformed configurations. Hence, the strain energy density for an incompressible Mooney-Rivlin material can be written as $\hat{V} = C_1(I_1 - 3) + C_2(I_2 - 3)$.

B. Pressure Work

The work done by the inflating gas with (gage) pressure P may be written as $\int P\,dV$, where the integral is performed over the volume enclosed by the inflated surface. This volume integral may be converted to a surface integral using Gauss theorem (at the mid-surface $x^3 = 0$) and expressed as [21]

$$W = \int\int \tfrac{1}{3}P\ y^i\ n_i\sqrt{\tilde{g}_s}\,dx^1 dx^2.$$

Using (2.1), the potential energy of the gas may be rewritten as

$$W = \int\int \tfrac{1}{6}P\varepsilon^{\alpha\beta}\varepsilon_{ijk}y^i\, y^j_{,\alpha}y^k_{,\beta}\sqrt{\tilde{g}_s}\,dx^1 dx^2. \quad (3.2)$$

C. Equilibrium

The total potential energy for the system is given by

$$\Pi = \int\int\left(-\hat{V} + \frac{1}{6h}PJ\varepsilon^{\alpha\beta}\varepsilon_{ijk}y^i y^j_{,\alpha}y^k_{,\beta}\right)h\sqrt{g_s}\,dx^1 dx^2, \quad (3.3)$$

where $J = \sqrt{\tilde{g}_s/g_s}$ and h is the undeformed thickness of the membrane. By the principle of minimum potential energy we have $\delta\Pi = 0$. Variation of Π gives (see [21])

$$\delta\Pi = \int\int\left[-\frac{\partial\hat{V}}{\partial y^i_{,\alpha}}\delta y^i_{,\alpha} - \frac{\partial\hat{V}}{\partial y^i}\delta y^i + \frac{1}{6h\sqrt{g}}Pe^{\alpha\beta}e_{ijk}\right.$$
$$\left. \times\left(\delta y^i y^j_{,\alpha}y^k_{,\beta} + y^i\delta y^j_{,\alpha}y^k_{,\beta} + y^i y^j_{,\alpha}\delta y^k_{,\beta}\right)\right]h\sqrt{g_s}\,dx^1 dx^2,$$
$$= \int\int\left[-\nabla_\alpha\left(\frac{\partial\hat{V}}{\partial y^i_{,\alpha}}\delta y^i\right) + \nabla_\alpha\left(\frac{\partial\hat{V}}{\partial y^i_{,\alpha}}\right)\delta y^i - \frac{\partial\hat{V}}{\partial y^i}\delta y^i\right.$$
$$\left. +\frac{1}{6h\sqrt{g}}Pe^{\alpha\beta}e_{ijk}\left(\delta y^i y^j_{,\alpha}y^k_{,\beta} + y^i\delta y^j_{,\alpha}y^k_{,\beta} + y^i y^j_{,\alpha}\delta y^k_{,\beta}\right)\right]$$
$$\times h\sqrt{g_s}\,dx^1 dx^2, \quad (3.4)$$

where ∇_α represents the covariant derivative with respect to x^α. Simplifying the expression $\delta\Pi$ using Gauss theorem, integration by parts and the properties of the permutation tensors gives

$$\delta\Pi = -\int_{\partial V}\frac{\partial\hat{V}}{\partial y^i_{,\alpha}}\delta y^i d\Sigma_\alpha + \int\int\left[\nabla_\alpha\left(\frac{\partial\hat{V}}{\partial y^i_{,\alpha}}\right)\delta y^i - \frac{\partial\hat{V}}{\partial y^i}\delta y^i\right.$$
$$\left. +\frac{1}{6h\sqrt{g}}Pe^{\alpha\beta}e_{ijk}\left(\delta y^i y^j_{,\alpha}y^k_{,\beta} - y^i_{,\alpha}\delta y^j y^k_{,\beta} - y^i_{,\beta}y^j_{,\alpha}\delta y^k\right)\right]$$
$$\times h\sqrt{g_s}\,dx^1 dx^2, \quad (3.5)$$

where $d\Sigma_\alpha$ is the differential length vector tangent to the boundary of the membrane ∂V. While the first term in (3.5) gives the boundary conditions, the second term yielding the

equation of equilibrium (3.5) is satisfied if and only if

$$\nabla_\alpha \left(\frac{\partial \hat{V}}{\partial y^i_{,\alpha}} \right) - \frac{\partial \hat{V}}{\partial y^i} + \frac{P}{h} J n_i = 0. \tag{3.6}$$

IV. GEOMETRY OF THE MEMBRANE

We consider axisymmetric membranes with three kinds of geometries, namely, the spherical, flat circular, and toroidal geometries. The spherical and flat geometries have positive and zero curvature, respectively, while the toroidal geometry has both positive and negative curvature regions with two zero-curvature boundaries.

Let r_s be the radius of the sphere, r_c be the radius of the flat circular membrane, and R and r_t be the major and minor radius of the toroid, respectively. We denote the field variables for the three geometries as u^i, which are defined conveniently for the individual cases later in this section. In the rest of the paper we will use the following nondimensional quantities. These are, for the spherical membrane,

$$(r, u^1) \to \frac{(r_s, u^1)}{h}, \quad \alpha \to \frac{C_2}{C_1}, \quad P \to \frac{P}{C_1},$$

for the flat circular membrane

$$(x^1, r, u^1, u^2) \to \frac{(x^1, r_c, u^1, u^2)}{h}, \quad \alpha \to \frac{C_2}{C_1}, \quad P \to \frac{P}{C_1},$$

and for the toroidal membrane

$$(r, u^1, u^2) \to \frac{(r_t, u^1, u^2)}{R}, \quad \alpha \to \frac{C_2}{C_1}, \quad P \to \frac{P R}{C_1 h}.$$

We also use the scaling $C_1 = 1$, $h = 1$, and $R = 1$. Thus, finally, the three nondimensional parameters in the problem are, namely, the geometric parameter r, the strain-hardening parameter α, and the inflation pressure P.

A. Spherical Membrane

Assuming a uniform radial inflation of the spherical membrane (see Fig. 1) with the inflation radius as u^1, the components of the undeformed and the deformed metric tensors can be written as

$$g_{ij} = \begin{pmatrix} r_s^2 & 0 & 0 \\ 0 & r_s^2 \sin^2 x^1 & 0 \\ 0 & 0 & 1 \end{pmatrix},$$
$$\tilde{g}_{ij} = \begin{pmatrix} (u^1)^2 & 0 & 0 \\ 0 & (u^1)^2 \sin^2 x^1 & 0 \\ 0 & 0 & \lambda_3^2 \end{pmatrix}. \tag{4.1}$$

The three principal stretches of the membrane are given by

$$\lambda_1 = \lambda_2 = \frac{u^1}{r_s}, \quad \lambda_3 = \frac{H}{h}, \tag{4.2}$$

where H is the deformed thickness.

The equilibrium solution for the spherical membrane is given by ([22,23])

$$P = \frac{4}{u^1} \left(1 - \frac{r^6}{(u^1)^6} \right) \left(1 + \alpha \frac{(u^1)^2}{r^2} \right). \tag{4.3}$$

For a given inflation pressure P, one can now solve the polynomial (4.3) for u^1, and thereby obtain the principal stretches from (4.2) for different strain-hardening and geometric parameters. At the pressure limit point, considering $u^1 = a_0$, we have the condition of local extremum,

$$\left. \frac{dP}{du^1} \right|_{u^1 = a_0} = 0. \tag{4.4}$$

Using (4.3) in (4.4), we obtain the condition

$$\alpha = \frac{z_0^2 (1 - 7 z_0^6)}{5 z_0^6 + 1}, \tag{4.5}$$

where $z_0 = r/a_0$. Substituting (4.5) in (4.3), the limit-point pressure of the spherical membrane can be calculated from the expression

$$r P_{\text{lim}} = \frac{8 z_0 (1 - z_0^6)^2}{5 z_0^6 + 1}. \tag{4.6}$$

It can be checked that the limit-point pressure does not exist beyond $\alpha = 0.2145$ (obtained by solving the equation $d\alpha/dz_0 = 0$). This analytical solution clearly shows that the first limit-point pressure is inversely proportional to the geometric parameter r and the proportionality constant is a function of the strain-hardening parameter α. The variation of the inflation pressure with the principal stretch of the spherical membrane for different strain-hardening parameters is shown in Fig. 2(a) for $r = 1$. The limit points for different strain-hardening parameters are traced by the dashed curve. It can be clearly observed from the dashed line that there is no limit-point pressure for the spherical membrane when the strain-hardening parameter exceeds $\alpha = 0.2145$. However, an inflexion point still exists. The variation of inflation pressure with the principal stretch of the spherical membrane for different geometric parameters and the strain-hardening parameter $\alpha = 0.1$ is shown in Fig. 2(b). It can be noted from the figure that with the increase in the value of the geometric parameter, the limit-point pressure reduces.

B. Circular Membrane

Two cases of circular flat membranes are considered in this paper: (a) a circular membrane with a fixed boundary as shown in Fig. 3(a), and (b) two circular flat membranes bonded at the boundary as shown in Fig. 3(b). Let the undeformed radii of the circular membranes be r_c, which are flat in their uninflated configuration as shown in Fig. 3, with x^1 along the radial direction. The deformed and the undeformed metric tensors on the circular membrane are given by [13]

$$g_{ij} = \begin{pmatrix} 1 & 0 & 0 \\ 0 & (x^1)^2 & 0 \\ 0 & 0 & 1 \end{pmatrix},$$
$$\tilde{g}_{ij} = \begin{pmatrix} \left((u^1_{,1})^2 + (u^2_{,1})^2 \right) & 0 & 0 \\ 0 & (u^1)^2 & 0 \\ 0 & 0 & \lambda_3^2 \end{pmatrix}. \tag{4.7}$$

where $u^1 = u^1(x^1)$ and $u^2 = u^2(x^1)$ are as shown in Fig. 5. The three principal stretches of the membrane are given
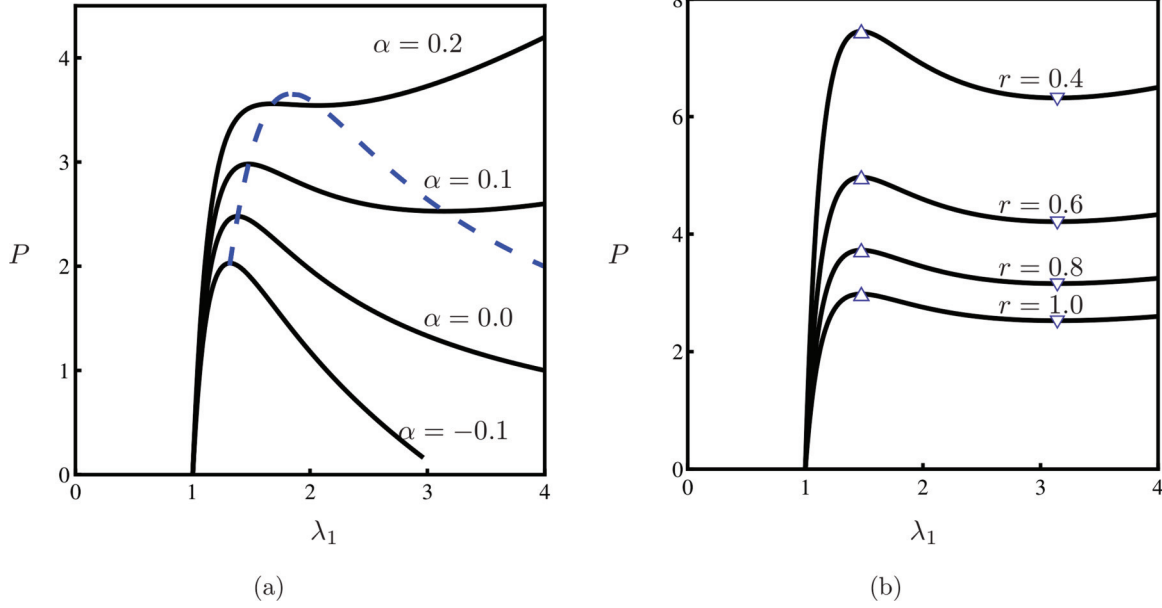
FIG. 2. (Color online) For a spherical membrane variation of (a) inflation pressure with principal stretch for different values of the material parameter and $r = 1$, and (b) inflation pressure with principal stretch for different values of the geometric parameter and $\alpha = 0.1$. Dashed curve in (a) traces the two limit-points of the membrane for different strain-hardening parameters and the markers in ($\triangle$, $\triangledown$) (b) represent the first and second limit points for different geometric parameters.

by

$$\lambda_1 = \sqrt{[(u^1_{,1})^2 + (u^2_{,1})^2]}, \quad \lambda_2 = \frac{u^1}{x^1}, \quad \lambda_3 = \frac{H}{h}. \quad (4.8)$$

(a)

(b)
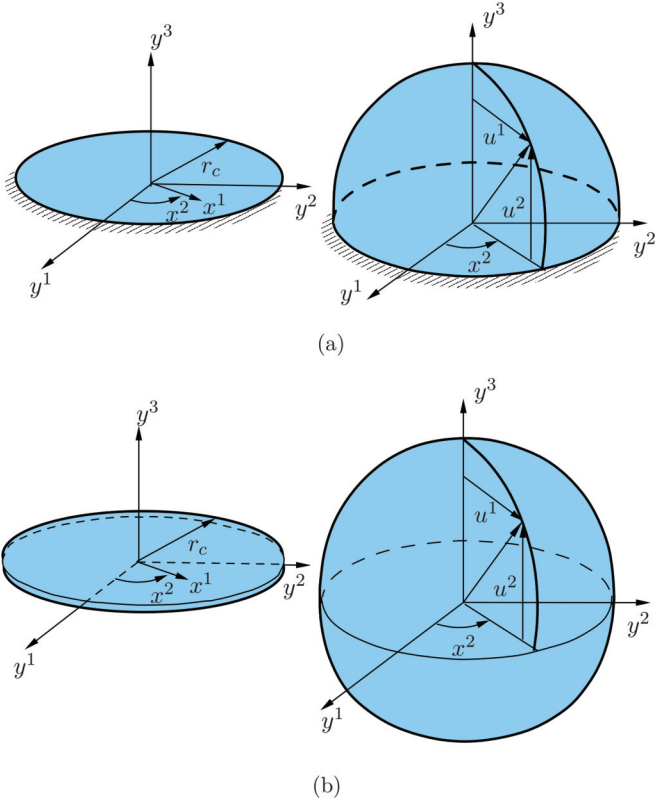
FIG. 3. (Color online) (a) Circular flat membrane fixed at the boundary before inflation and after inflation. (b) Configurations before and after inflation of two circular flat membranes made of the same material bonded at the boundary.

The equilibrium equations of the circular membrane may be represented as [11]

$$\mathbf{F}(u^i_{,1}, u^i, x^1, P) = \mathbf{0}. \quad (4.9)$$

Following [24] and [13], it can be observed that the equilibrium equations (4.9) obey the scaling property $\mathbf{F}(u^i_{,1}, \delta u^i, \delta x^1, P/\delta) = \mathbf{F}(u^i_{,1}, u^i, x^1, P)$. This invariance property can be used to easily solve the inflation problem with the conditions $\lambda_1|_{x^1=0} = \lambda_2|_{x^1=0} = \lambda_0$ along with the boundary conditions for the two cases as follows:

A boundary fixed circular membrane:
$$u^1(0) = 0, u^2_{,1}(0) = 0, u^1(r) = 0, \quad (4.10)$$

Two bonded circular membranes:
$$u^1(0) = 0, u^2_{,1}(0) = 0, u^1_{,1}(r) = 0. \quad (4.11)$$

The variation of the principal stretches of the membrane(s) at $x^1 = 0$ for $\alpha = -0.1, 0, 0.1, 0.2$ and two inflated configurations at pressure $P = 3$ for $\alpha = 0$ before and after the limit-point pressure are presented in Fig. 4 (for a circular flat membrane) and Fig. 5 (for two bonded circular membranes). For the case of bonded circular membranes, impending wrinkling conditions of the membrane have been checked following [25]. We have observed (results not presented) for this case that there is no wrinkling beyond a certain value of the inflation pressure.

C. Toroidal Membrane

Consider a toroidal membrane of ring radius R and cross-sectional radius r_t with coordinates x^1 (meridional) and x^2 (circumferential) on the surface as shown in Fig. 6. The deformed and the undeformed metric tensors on the toroidal

(a)

(b)
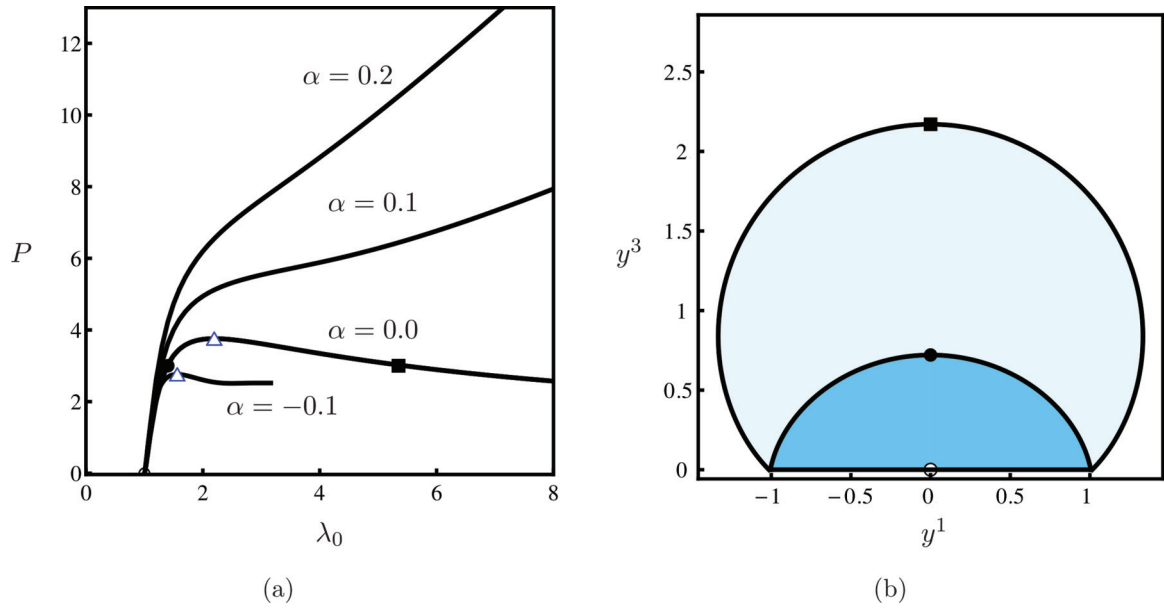
FIG. 4. (Color online) (a) Variation of inflation pressure with the principal stretches ($\lambda_1 = \lambda_2 = \lambda_0$) with $r = 1$ at $x^1 = 0$ for strain-hardening parameter $\alpha = -0.1, 0, 0.1, 0.2$. (b) Two inflated configurations at $P = 3$ and $\alpha = 0$ for a circular membrane fixed at the boundary on a $y^1 - y^3$ plane. The principal stretch values corresponding to the markers ($\bigcirc$, $\bullet$, $\blacksquare$) shown in (b) are marked in (a). The marker ($\triangle$) in (a) represents the first limit point.

membrane are given by ([12,25])

$$
g_{ij} = \begin{pmatrix} r_t^2 & 0 & 0 \\ 0 & (R + r_t \cos x^1)^2 & 0 \\ 0 & 0 & 1 \end{pmatrix},
$$
$$
\tilde{g}_{ij} = \begin{pmatrix} \left[(u_{,1}^1)^2 + (u_{,1}^2)^2 \right] & 0 & 0 \\ 0 & (u^1)^2 & 0 \\ 0 & 0 & \lambda_3^2 \end{pmatrix}.
$$
(4.12)

The three principal stretches of the toroidal membrane are given by

$$
\lambda_1 = \frac{\sqrt{\left[(u_{,1}^1)^2 + (u_{,1}^2)^2 \right]}}{r_t},
$$
$$
\lambda_2 = \frac{u^1}{(R + r_t \cos x^1)},
$$
(4.13)
$$
\lambda_3 = \frac{H}{h}.
$$

(a)

(b)
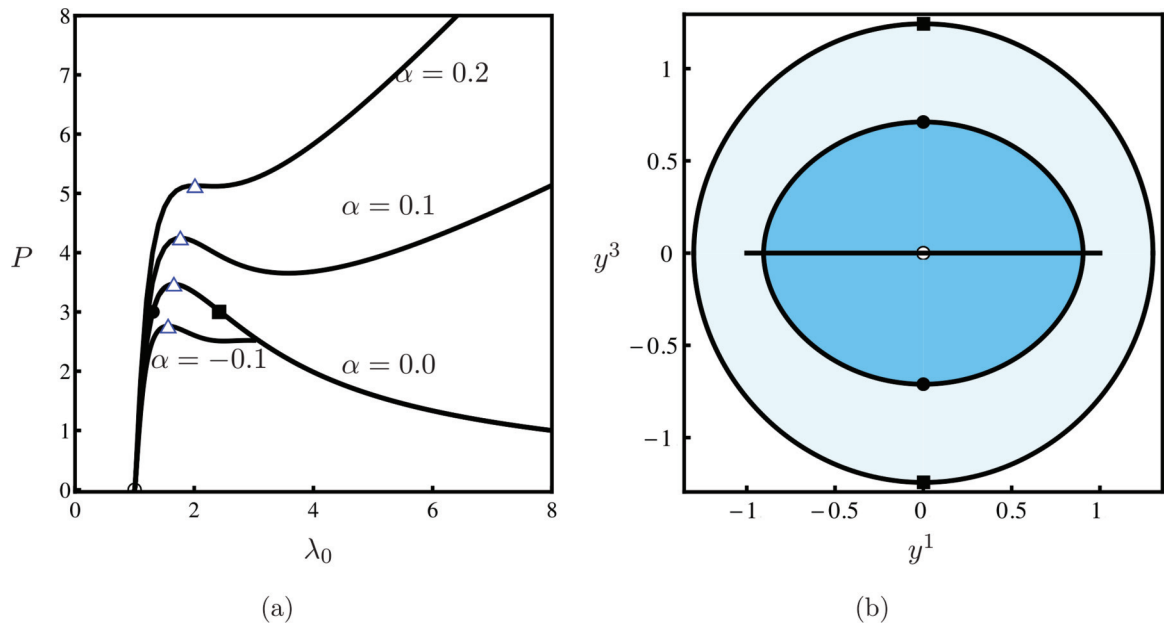
FIG. 5. (Color online) (a) Variation of inflation pressure with the principal stretches ($\lambda_1 = \lambda_2 = \lambda_0$) at $x^1 = 0$ for $r = 1$. (b) Two inflated configurations at $P = 3$ and $\alpha = 0$ for the case of two circular membranes bonded at the boundary on a $y^1 - y^3$ plane. The principal stretch values corresponding to the markers ($\bigcirc$, $\bullet$, $\blacksquare$) shown in (b) are marked in (a). The marker ($\triangle$) in (a) represents the first limit point.
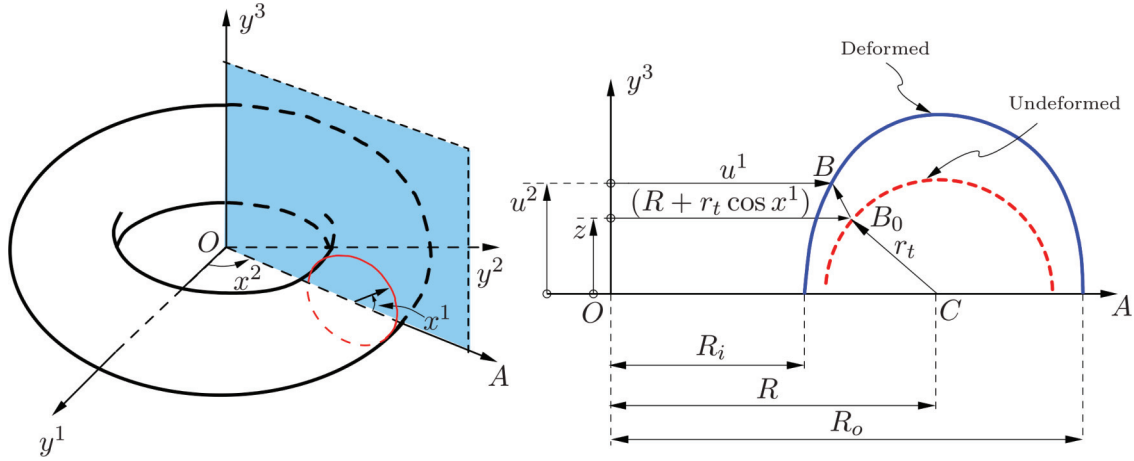
FIG. 6. (Color online) Toroidal membrane before inflation and after inflation.

The equilibrium equations of the toroidal membrane are obtained from (3.6) as

$$
\frac{d}{dx^1}\left[\frac{\partial\lambda_1^2}{\partial u_{,1}^1}\left(1+\alpha\lambda_2^2\right)\left(1-\frac{1}{\lambda_1^4\lambda_2^2}\right)\sqrt{g_s}\right]
$$
$$
-\frac{\partial\lambda_2^2}{\partial u^1}\left(1+\alpha\lambda_1^2\right)\left(1-\frac{1}{\lambda_1^2\lambda_2^4}\right)\sqrt{g_s}+Pu^1\,u_{,1}^2=0,\quad(4.14)
$$
$$
\frac{d}{dx^1}\left[\frac{\partial\lambda_1^2}{\partial u_{,1}^2}\left(1+\alpha\lambda_2^2\right)\left(1-\frac{1}{\lambda_1^4\lambda_2^2}\right)\sqrt{g_s}-\frac{1}{2}P(u^1)^2\right]=0.
$$
$$
(4.15)
$$

From the symmetry conditions of the membrane, the boundary conditions may be written as

$$
u_{,1}^1(0)=u_{,1}^1(\pi)=0,\quad u^2(0)=u^2(\pi)=0.\quad(4.16)
$$

The two-point boundary value problem of the membrane defined by (4.14)–(4.16) is solved using a shooting method as detailed in Ref. [12].

The variations of principal stretches of the toroidal membrane at $x^1=0$ for strain-hardening parameter $\alpha=-0.1,0,0.1,0.2$ are shown in Fig. 7(a) and the two inflated configurations of the torus cross section at pressure $P=2.9$ for $\alpha=0.1$ before and after the limit point are shown in Fig. 7(b). In this case the impending wrinkling conditions of the membrane have also been checked following [25].

V. LIMIT-POINT INSTABILITY

Consider a small circular patch (not necessarily flat) of radius r in the uninflated membrane which deforms to a radius $\tilde{r}$ upon inflation. Let P be the corresponding pressure acting
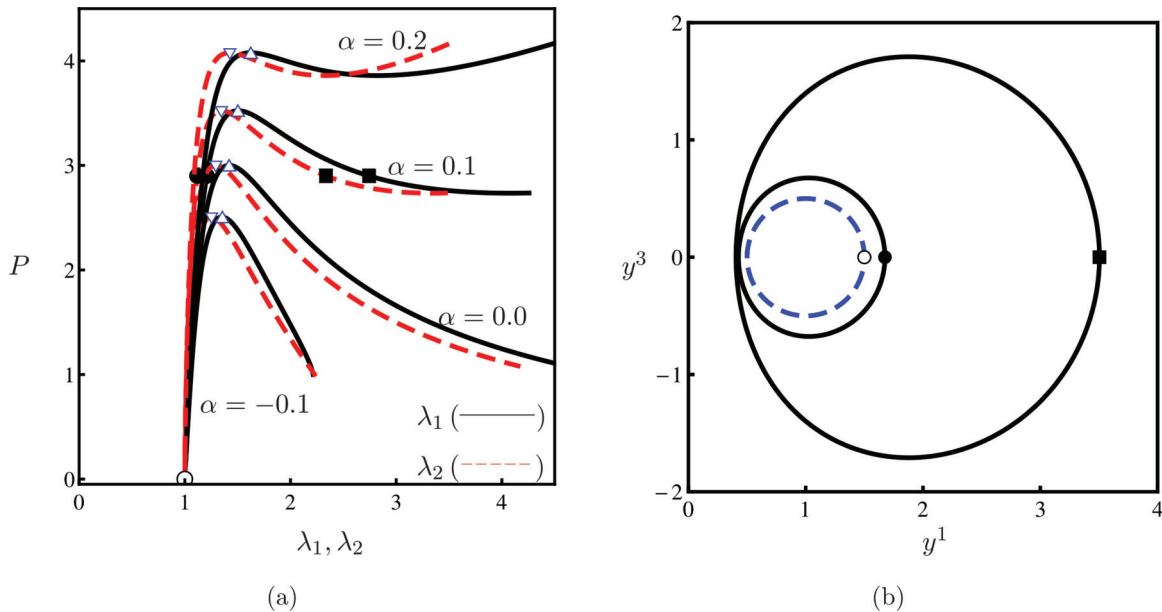
FIG. 7. (Color online) (a) Variation of inflation pressure with the principal stretches (λ_1,λ_2) at $x^1=0$ for the strain-hardening parameter $\alpha=-0.1,0,0.1,0.2$. (b) Two inflated configurations at $P=2.9$ and $\alpha=0.1$ for the case of a toroidal membrane on a y^1-y^3 plane. The principal stretch values corresponding to the markers ($\bigcirc,\bullet,\blacksquare$) shown in (b) are marked in (a). The markers ($\triangle,\triangledown$) in (a) represent the first limit points corresponding to (λ_1,λ_2).
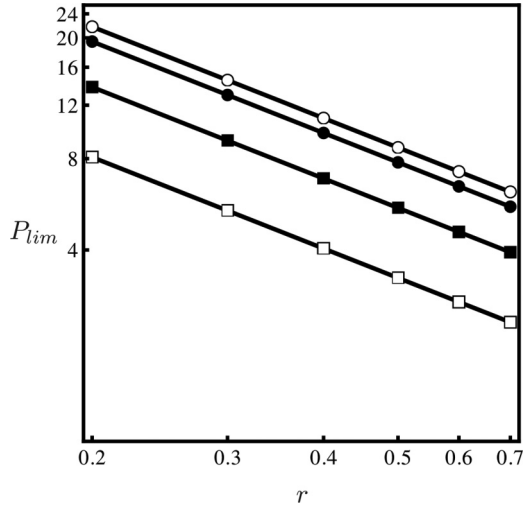
FIG. 8. Variation of the limit-point pressure with geometric parameter in the log-log plane circular membrane with fixed boundary ($\bigcirc$), two circular membranes bonded at the boundary ($\bullet$), spherical membrane ($\blacksquare$), and toroidal membrane ($\square$).

on the patch. Assuming the equibiaxial state of stretch, $\lambda_1 = \lambda_2 = \lambda = \tilde{r}/r$. For a given strain energy density function $\hat{V}$, the stress resultant is given by $T = (h/\lambda)\partial\hat{V}/\partial\lambda$. The relation between the pressure and the stress resultant can be written up to the first order in thickness of the membrane (for thin shell approximation) as

$$P A \sim T L, \tag{5.1}$$

where $A \propto \tilde{r}^2$ and $L \propto \tilde{r}$ are, respectively, the projected surface area and circumference of the patch. One may rewrite (5.1) as

$$P\lambda^2 r^2 \sim T\lambda r \Rightarrow Pr \sim \frac{h}{\lambda^2}\frac{\partial\hat{V}}{\partial\lambda}. \tag{5.2}$$

Now, at the limit point, one can write (from the local extremum condition of the stress-stretch relation (see, e.g., [3,17,26])

$$\frac{-2}{\lambda^3}\frac{\partial\hat{V}}{\partial\lambda} + \frac{1}{\lambda^2}\frac{\partial^2\hat{V}}{\partial\lambda^2} = 0. \tag{5.3}$$

Integrating (5.3) once gives

$$\frac{1}{\lambda^2}\frac{\partial\hat{V}}{\partial\lambda} = I, \tag{5.4}$$

where I is the integration constant. Using (5.4) in (5.2) at the limit-point pressure yields the relation

$$r P_{\text{lim}} = \Gamma, \tag{5.5}$$

where Γ is a constant (obtained by a scaling of I) which depends only on the geometry and the material parameters involved in the strain energy function of the membrane. Here, the only material parameter is the strain-hardening parameter α.

To check the relation (5.5), the values of the limit-point pressure are obtained for four different geometries with the Mooney-Rivlin strain energy function. The variation of the limit-point pressure P_{lim} for $\alpha = 0.05$ with the geometric parameter r is shown on the log-log plane in the Fig. 8 for different geometries of the membrane. For all the geometries, all the points fall on respective straight lines, all of which have a slope of -1, as observed in Fig. 8. Thus P_{lim} is inversely proportional to the geometric parameter given by (5.5) (where Γ is the x intercept in Fig. 8). It is interesting to note that for the case of the toroidal membrane, the limit-point pressure is independent of the major radius R of the torus. As mentioned above, it is evident that Γ can only be a function of the strain-hardening parameter α. A plot of Γ with $(1 + \alpha)$ is shown on the log-log plane in Fig. 9(a) for different geometries. For all the geometries considered, all the points of the respective geometries match excellently with the corresponding straight line fits. However, the slope and y

(a)

(b)
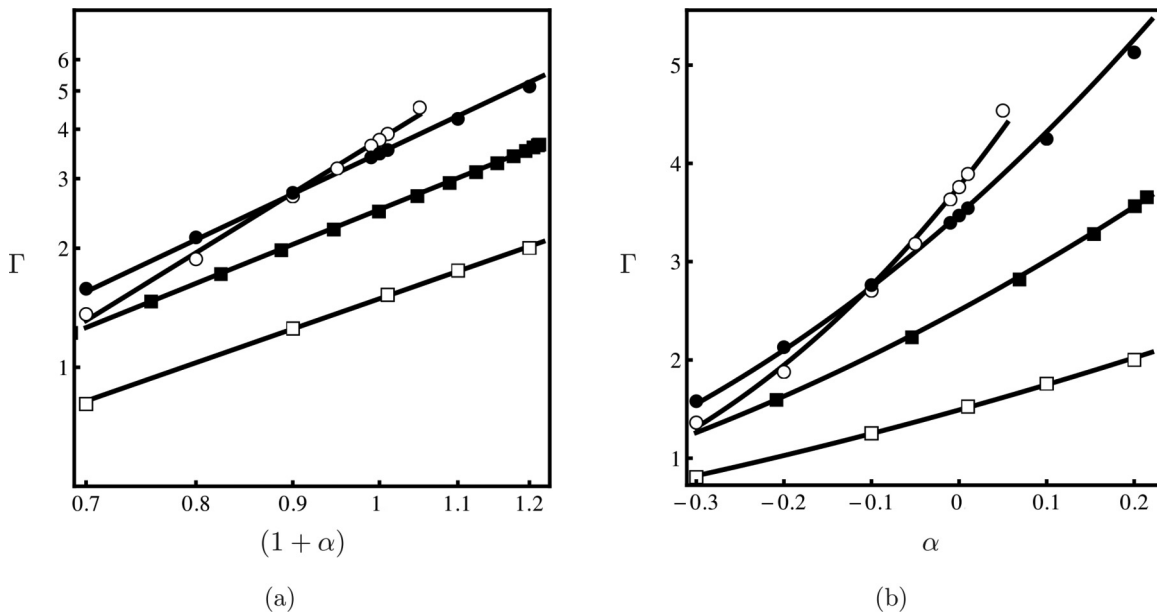
FIG. 9. Variation of proportionality constant Γ with strain-hardening parameter (α) for circular membrane with fixed boundary ($\bigcirc$), two circular membranes bonded at the boundary ($\bullet$), spherical membrane ($\blacksquare$), and toroidal membrane ($\square$).

TABLE I. Constants for the power-law relation $\Gamma = a(1 + \alpha)^b$ for different geometries.

Geometry	a	b
Circular membrane fixed at the boundary	3.7664	2.9559
Two circular membranes bonded at the boundary	3.4819	2.2645
Spherical membrane	2.5053	1.9261
Toroidal membrane	1.4910	1.6703

intercept of these lines vary with the geometry. This clearly indicates the power-law dependence of Γ on α, which can be expressed as

$$\Gamma = a(1 + \alpha)^b,$$

where a and b are suitable constants. The variation of Γ with α for different geometries is shown in Fig. 9(b). The constants a and b obtained from the intercept and the slope of these lines in Fig. 9(a) for different geometries are given in Table I. These constants are universal for the corresponding geometry. Using the above table, one can now easily find the limit-point inflation pressure of the four membrane geometries considered.

VI. CONCLUSIONS

The phenomenon of limit-point instability during finite inflation of hyperelastic membranes under internal pressure is addressed in this paper. The Mooney-Rivlin material model for the membrane is considered in the analysis. Four axisymmetric membrane geometries are studied, namely, a spherical membrane, a circular membrane fixed at the boundary, two circular membranes bonded at the periphery, and a toroidal membrane.

In the vicinity of a limit pressure point, a dramatic change in the inflation behavior of a membrane is expected. Any imperfection or defect in the material may lead to unpredictable behavior of the structure (including the possibility of bursting). Therefore, *a priori* estimation of the limit-point pressure assumes importance. A functional relationship of a general form relating the limit-point instability pressure with a geometric parameter of the uninflated membrane has been proposed. For the different cases, the geometry-dependent parameters in the functional relationship have been obtained numerically. These are expected to be useful in the estimation of the limit-point pressure for the geometries considered.

The dependence of the limit-point pressure on the geometry is due to the connection of the geometry with the stress distribution. However, what is remarkable is that the limit-point pressure depends on a geometric parameter of the uninflated membrane. This functional dependence appears to be an invariant property of the membrane geometry for the Mooney-Rivlin class of hyperelastic materials. It remains to be seen how the constants can be related in a more fundamental way to the geometry of the membrane. Furthermore, the role of geometry on the small-amplitude dynamics and stability of the membranes around the critical points may be interesting to investigate (see, e.g., [27,28]).

[1] M. Mooney, J. Appl. Phys. **11**, 582 (1940).

[2] L. R. G. Treloar, *The Physics of Rubber Elasticity*, Oxford Classic Texts in the Physical Sciences (Clarendon Press, Oxford, 1975).

[3] R. W. Ogden, *Non-linear Elastic Deformations* (Ellis-Horwood, Chichester, U.K., 1984).

[4] Y. C. Fung, *An Introduction to the Theory of Aeroelasticity*, Phoenix Edition Series (Dover, Mineola, NY, 2002).

[5] R. S. Rivlin, Philos. Trans. R. Soc. London A **240**, 459 (1948).

[6] R. S. Rivlin, Philos. Trans. R. Soc. London A **240**, 491 (1948).

[7] J. E. Adkins and R. S. Rivlin, Philos. Trans. R. Soc. London A **244**, 505 (1952).

[8] A. E. Green and J. E. Adkins, *Large Elastic Deformation* (Oxford University Press, London, 1970).

[9] P. M. Naghdi, *The Theory of Shells and Plates, S. Flügge's Handbuch der Physik*, Vol. VIa/2, edited by C. Truesdell (Springer, Berlin, 1972).

[10] P. M. Naghdi and P. Y. Tang, Philos. Trans. R. Soc. London A **287**, 145 (1977).

[11] A. E. Green and W. Zerna, *Theoretical Elasticity* (Dover, New York, 1992).

[12] G. Tamadapu and A. DasGupta (unpublished).

[13] A. Patil and A. DasGupta, Eur. J. Mech. A. Solids **41**, 28 (2013).

[14] A. Needleman, Int. J. Solids Struct. **13**, 409 (1977).

[15] W. Dreyer, I. Müller, and P. Strehlow, Q. J. Mech. Appl. Math. **35**, 419 (1982).

[16] H. Alexander, Int. J. Eng. Sci. **9**, 151 (1971).

[17] L. M. Kanner and C. O. Horgan, Int. J. Non Linear Mech. **42**, 204 (2007).

[18] *Gossamer Spacecraft: Membrane and Inflatable Structures Technology for Space Applications*, edited by C. H. M. Jenkins (AIAA, Reston, VA, 2001), Vol. 191.

[19] J. Janáček and V. Vojta, J. Polym. Sci.: Polym. Symp. **53**, 291 (1975).

[20] A. F. Bower, *Applied Mechanics of Solids* (Taylor & Francis, London, 2011).

[21] D. J. Steigmann, Proc. R. Soc. London A **429**, 141 (1990).

[22] H. O. Foster, Int. J. Eng. Sci. **5**, 95 (1967).

[23] A. Eriksson and A. Nordmark, Comput. Methods Appl. Mech. Eng. **237**, 118 (2012).

[24] W. H. Yang and W. W. Feng, J. Appl. Mech. **37**, 1002 (1970).

[25] G. Tamadapu and A. DasGupta, Int. J. Non Linear Mech. **49**, 31 (2013).

[26] A. Goriely, M. Destrade, and M. Ben Amar, Q. J. Mech. Appl. Math. **59**, 615 (2006).

[27] G. Tamadapu and A. DasGupta, Int. J. Eng. Sci. **60**, 25 (2012).

[28] A. DasGupta and G. Tamadapu, Eur. J. Mech. A Solids **39**, 280 (2013).